Hindawi
Geofluids
Volume 2023, Article ID 9357711, 12 pages
https://doi.org/10.1155/2023/9357711

Research Article

Insights into Enhanced Oil Recovery by Coupling Branched-Preformed Particle Gel and Viscosity Reducer Flooding in Ordinary Heavy Oil Reservoir

Zongyang Li

Research Institute of Exploration and Development of Shengli Oilfield, SINOPEC, Dongying 257000, China

Correspondence should be addressed to Zongyang Li; lizongyang1108@163.com

Received 8 November 2022; Revised 16 December 2022; Accepted 27 March 2023; Published 30 June 2023

Academic Editor: Shixun Bai

Viscosity reducer flooding has been successfully applied in tertiary oil recovery of ordinary heavy oil reservoirs. However, lowering interfacial tension or reducing oil viscosity, which is more critical for viscosity reducer to improve oil recovery of ordinary heavy oil, has not yet formed a unified understanding, which restricts the further large-scale application of viscosity reducer flooding for ordinary heavy oil reservoir. Moreover, when the dominant water flow channel is formed in the reservoir, the sweep efficiency decreases sharply and can affect oil recovery efficiency of viscosity reducer. Therefore, in this study, the concept of branched-preformed particle gel (B-PPG) coupling viscosity reducer flooding is proposed. The oil-water interfacial tension performance, emulsification ability, and viscosity reduction performance of three different viscosity reducers were evaluated. The enhanced oil recovery ability of viscosity reducers, B-PPG, and viscosity reducer/B-PPG composite systems was investigated by performing sand pack flooding experiments. The results show that the oil-water interfacial tensions of the three viscosity reducers S1, S2, and S3 are $0.432\,mN{\cdot}m^{-1}$, $0.0112\,mN{\cdot}m^{-1}$, and $0.0031\,mN{\cdot}m^{-1}$, respectively. S1 with the highest interfacial tension has the best emulsification and viscosity reduction performance, S2 is the second, and S3 is the worst. The lower the interfacial tension, the worse the emulsification stability. The sand pack flooding results show that the incremental oil recovery of viscosity reducer S2 flooding is the largest, 7.5%, followed by S1, 7.3%, and S3, 5.6%. The viscosity reducer S2 with moderate interfacial tension and emulsifying capacity has the best ability to improve the recovery of ordinary heavy oil. The incremental oil recovery of B-PPG is 12.7%, which is significantly higher than that of viscosity reducer flooding. Compared with viscosity reducing flooding, the viscosity reducer/B-PPG composite systems have better enhanced oil recovery capacity. The findings of this study can help for better understanding of enhancing oil recovery for ordinary heavy oil reservoir.

1. Introduction

With the continuous development of petroleum industry, the proportion of heavy oil in the world's remaining oil resources is increasing. Heavy oil exploitation has a significant impact on the pattern of world oil production. However, heavy oil has the characteristics of high colloid and asphaltene content, high viscosity and density, and poor flow capacity, resulting in great difficulty and high production cost of recovering heavy oil [1–4]. For ordinary heavy oil reservoirs, due to adverse mobility ratio between water and oil, the fingering effect occurs and the oil recovery efficiency of conventional water flooding is low. To improve oil recovery efficiency of heavy oil reservoirs, thermal oil recovery technologies including steam huff and puff, steam flooding, and steam-assisted gravity drainage (SAGD) have been applied. The thermal oil recovery methods focus on reducing the viscosity of heavy oil by destroying the supramolecular structure between colloid and asphaltene in heavy oil and reducing the water-oil mobility ratio, which enlarges the sweep efficiency and improves oil recovery [5–11]. However, due to high consumption of energy and water to generate steam and severe heat loss, the thermal methods are economically nonprofitable for the deep and thin heavy oil reservoirs [12–15]. Therefore, it is of great significance to change the development mode of ordinary heavy oil and achieve highly efficient development of ordinary heavy oil reservoir.

The nonthermal oil recovery technology, especially chemical flooding technology, has attracted more and more attention because of its wide reservoir application range and low economic cost, which has been successfully applied in many heavy oil reservoirs [16–23]. Viscosity reducing production is one of the most commonly used methods for recovering heavy oil in ordinary heavy oil reservoir. The main enhanced oil recovery (EOR) mechanisms for viscosity reducing production can be mainly divided into two aspects: On the one hand, through the emulsification of viscosity reducer under certain external force conditions, the heavy oil is dispersed into formation water and forms relatively stable O/W emulsion, which can greatly reduce the viscosity of heavy oil and improve its fluidity in porous media. On the other hand, it can effectively reduce the adhesion work by reducing the interfacial tension between oil and water, so as to reduce the flow resistance of crude oil and improve the oil displacement efficiency [24–26]. However, the two different EOR mechanisms including emulsifying viscosity reduction and lower oil-water interfacial tension, which is more critical for viscosity reducer to improve oil recovery of ordinary heavy oil, have not yet formed a unified understanding. Some researchers believe that the interfacial tension is the primary index to determine the performance of viscosity reducer. Lower interfacial tension can effectively reduce the residual oil saturation [27–30]. Some researchers also believe that the mechanism of emulsification and viscosity reduction is the key to greatly improve the recovery of ordinary heavy oil. The viscosity reducer with better emulsification ability and viscosity reduction performance has better EOR effect [31–33].

In addition, due to the high viscosity of heavy oil and water-oil mobility ratio, the viscosity reducer flooding is not satisfied. In order to reduce this deficiency, researchers have proposed combined flooding systems such as viscosity reducer/polymer or viscosity reducer/alkali [34–38]. Polymer can increase the viscosity of injection water and reduce water-oil mobility ratio and thus expand sweep volume. The alkali can react with crude oil to form in situ surfactant, which can promote the formation of O/W emulsion and reduce the viscosity. The formation of in situ surfactant can reduce oil-water interfacial tension and improve oil displacement efficiency. Alkali-containing systems often have serious scaling problems, which restricts the development of alkali/surfactant binary flooding [39–43]. The range of crude oil viscosity used in the conventional viscosity reducer/polymer combined system is limited, resulting in low recovery and unable to realize the efficient development of the conventional heavy oil reservoir. Moreover, when the dominant water flow channel is formed in the reservoir, the sweep efficiency decreases sharply and can affect the enhanced oil recovery ability.

Therefore, to improve the sweep efficiency, the branched-preformed particle gel (B-PPG) was developed by Shengli Oilfield, which has unique "partial crosslinking and partial branching" molecular structures. The B-PPG has viscoelastic properties, which can plug the dominant water flow channel, change the subsequent flow direction, and enlarge the swept volume. The B-PPG can have better sweep efficiency improvement ability than polymer solution [44–52]. Thus, in this study, the concept of branched-preformed particle gel (B-PPG) coupling viscosity reducer flooding is proposed firstly. To determine which mechanism dominates for viscosity reducer flooding and clarify EOR efficiency by coupling B-PPG and viscosity reducer, a series of experiments including physicochemical property evaluation of viscosity reducer and sand pack flooding experiments was systematically conducted in this study. Firstly, three different viscosity reducers with different interfacial tension and emulsification ability were collected. Then, the oil-water interfacial tension performance, emulsification performance, and viscosity reduction performance were studied. Finally, a series of sand pack flooding experiments was performed to investigate the EOR ability of three different viscosity reducers, B-PPG, and viscosity reducer/B-PPG composite systems. In general, we hope that this study can clarify the contribution of interfacial tension performance and emulsification performance of viscosity reducer to enhance oil recovery of common heavy oil and provide a new idea for enhancing oil recovery of common heavy oil.

Table 1: The ionic composition and concentration of formation brine.

Ionic composition	Na^+	Ca^{2+}	Mg^{2+}	Cl^-
Concentration ($mg \cdot L^{-1}$)	3667	292	65	6583

2. Materials and Methods

2.1. Materials. The viscosity reducers used in this study were nonionic surfactants (S1, S2, and S3) provided by Yangzhou Runda Co., Ltd. The B-PPG used in this study was the branched-preformed particle gel provided by Shengli Oilfield. The elastic modulus and median particle size (D50) of B-PPG were 4.3 Pa and 506.5 μm, respectively.

At 70°C, the density and viscosity of heavy oil obtained from Shengli Oilfield are $0.982\,g \cdot cm^{-3}$ and $2570\,mPa \cdot s$, respectively. The ionic composition and concentration of simulated formation brine with TDS of $10607\,mg \cdot L^{-1}$ are listed in Table 1.

2.2. Methods

2.2.1. Oil-Water Interfacial Tension Measurement. The oil-water interfacial tension between three different viscosity reducers and degassed heavy oil in chen25 block of Shengli Oilfield was measured by spinning drop method on Texas-500c interface tension meter. The measured temperature was 70°C, and the rotating speed was $5000\,r \cdot min^{-1}$.

2.2.2. Emulsification Stability Evaluation. Emulsification stability is one of the important indexes to evaluate the performance of viscosity reducers. The emulsification stability is often determined by the water separating proportion referring to the percentage of the volume of water separated from

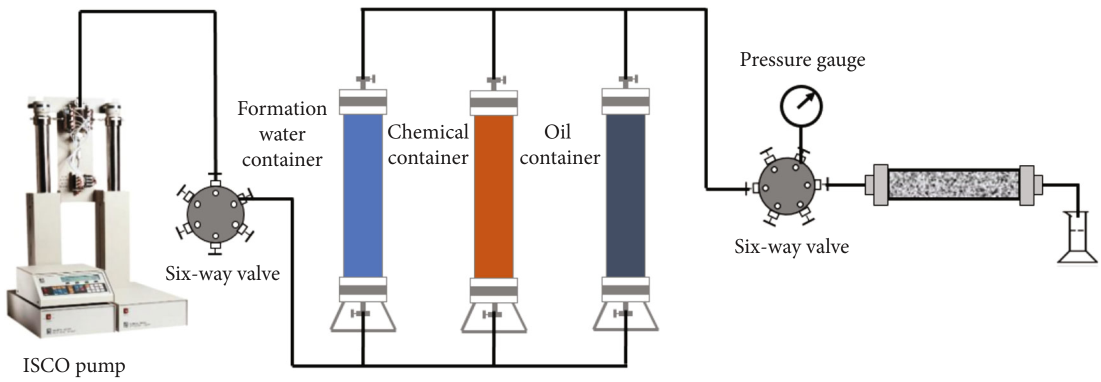

Figure 1: The schematic diagram of sand pack flooding experimental apparatus.

the emulsion. It is a commonly used quantitative evaluation index to evaluate the emulsification stability of viscosity reducers. The higher the water separating proportion, the worse the emulsification stability of viscosity reducer. The experimental procedures of emulsification stability evaluation were as follows: (1) The prepared viscosity reducer with concentration of 3000 mg·L^{-1} and heavy oil were placed in a 70°C oven for 2.0 h. (2) Then, according to the oil-water ratio of 3 : 7, the heavy oil and viscosity reducer solution were stirred with a homogenizer for 3 min at the speed of 3000 r·min^{-1} to form O/W emulsion. (3) The formed emulsion was placed in the 10 mL plugged test tube at 70°C constant temperature water bath and started timing at the same time. The position of oil-water interface and the volume of separated water in the test tube were recorded at regular intervals, and the water separating proportion of emulsion at different times was calculated according to the following equation:

$$f_1 = \frac{V_w}{V_0}, \tag{1}$$

where f_1 is the water separating proportion (%), V_w is the water separating volume (mL), and V_0 is the initial water volume (mL).

2.2.3. The Viscosity Reduction Ability Evaluation. Different viscosity reducer (S1, S2, and S3) solutions with concentration of 3000 mg·L^{-1} were prepared by simulated formation brine. Then, according to the oil-water ratio of 3 : 7, the predetermined amount of surfactant and heavy oil was stirred with a homogenizer for 3 min at different speeds of 500 r·min^{-1}, 1000 r·min^{-1}, and 3000 r·min^{-1} to form emulsion. At 70°C, the viscosity of formed emulsion was measured by Brookfield DV-II viscometer, and the viscosity reduction rate of heavy oil emulsification at this time was calculated according to the following equation:

$$f_2 = \frac{\mu_0 - \mu}{\mu_0}, \tag{2}$$

where f_2 is the viscosity reduction rate (%), μ_0 is the viscosity of heavy oil (mPa·s), and μ is the viscosity of formed emulsion (mPa·s).

Table 2: The porosity and permeability of sand packs used for flooding experiments.

No.	Chemical slug	Permeability (μm^2)	Porosity (%)
1#	3000 mg·L^{-1} S1	1.1	42.2
2#	3000 mg·L^{-1} S2	1.1	41.4
3#	3000 mg·L^{-1} S3	1.0	40.8
4#	800 mg·L^{-1} B-PPG	1.0	40.8
5#	3000 mg·L^{-1} S1+800 mg·L^{-1} B-PPG	1.0	40.8
6#	3000 mg·L^{-1} S2+800 mg·L^{-1} B-PPG	1.0	41.4
7#	3000 mg·L^{-1} S3+800 mg·L^{-1} B-PPG	0.9	40.8

2.2.4. The Morphology of Formed Emulsion Observation. To grasp a better understanding on the mechanism of surfactant emulsification and viscosity reduction, the morphology of formed emulsion at different rotating speeds was studied by optical microscope. The Axioskop 40 microscope (Carl Zeiss) enables us to analyze samples placed between slide and cover glass under ordinary light and polarized light.

The experimental procedures were as follows: (1) The viscosity reducer solution and crude oil were placed in an incubator water bath at 70°C for 3 h. (2) Then, heavy oil and viscosity reducer solution was mixed evenly according to the oil-water ratio of 3 : 7 and emulsified it with a dispersion homogenizer at different speeds of 500 r/min, 1000 r/min, and 3000 r/min for 3 min. In the emulsification process, the beaker was placed in a 70°C constant temperature water bath. (3) The formed emulsion was placed on the glass slide, and the morphology of the emulsion was observed by microscope.

2.2.5. Sand Pack Flooding Experiment. In order to investigate the EOR ability of three different viscosity reducers, B-PPG and coupling B-PPG, and viscosity reducers, a series of sand pack flooding experiments was carried out. Figure 1 depicts the schematic diagram of sand pack flooding oil

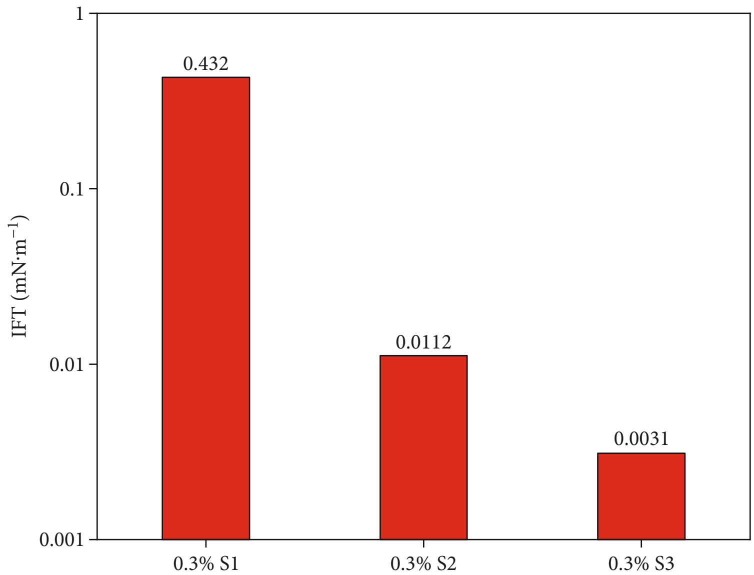

Figure 2: IFT between different viscosity reducers and heavy oil.

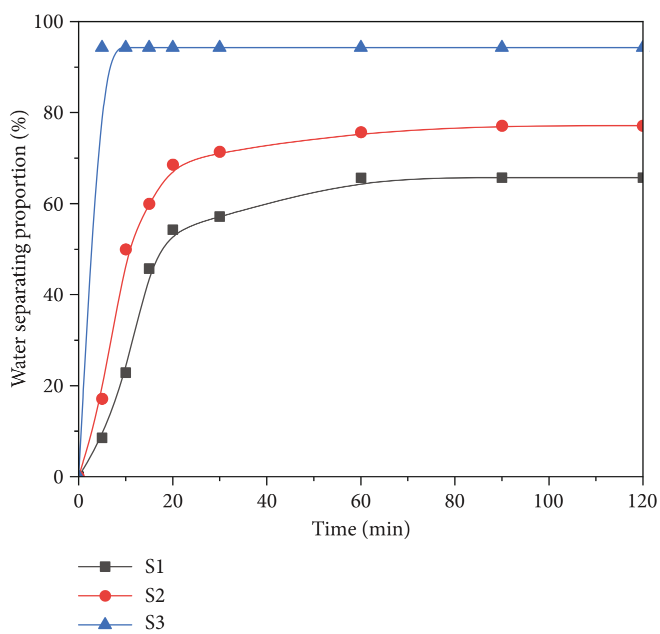

Figure 3: The water separating proportion of different viscosity reducers versus time.

experimental apparatus. The flooding experiments were carried out at 70°C and atmospheric pressure. The experimental processes were as follows: (1) sand pack preparation and the measurement of permeability: the sand pack was filled with 120~140 mesh quartz sand by wet packing method, and the liquid permeability was measured at the water flooding rate of 1.0 mL/min; (2) crude oil saturation period: the wet-packed sand pack was flooded with crude oil at the rate of 0.1 mL/min until complete oil production at 80°C. Then, the sand pack was sealed and put in the oven at 70°C for aging for 48 h after saturated oil; (3) water flooding and chemical flooding period: the initial water flooding was conducted until the water cut reached 95% at the flooding rate of 0.3 mL/min. Then, 0.4 PV different chemical slugs were injected into the sand packs; (4) subsequent water flooding period: the subsequent water flooding was conducted until the water cut reached 98%. Then, the flooding experiments were terminated. The injection pressure and volume of produced water and oil were recorded at different flooding periods. Table 2 shows the porosity and permeability properties of sand packs used for flooding experiments.

Table 3: Viscosity reduction rate of three viscosity reducers at different shear rates at 70°C.

Chemical slug	Oil-water volume ratio	Shear rate ($r \cdot min^{-1}$)	Crude oil viscosity (mPa·s)	Emulsion viscosity (mPa·s)	Viscosity reduction rate (%)
S1	3 : 7	500	2570	272	89.4
S1	3 : 7	1000	2570	187	92.7
S1	3 : 7	3000	2570	46	98.2
S2	3 : 7	500	2570	421	87.6
S2	3 : 7	1000	2570	241	90.6
S2	3 : 7	3000	2570	127	95.1
S3	3 : 7	500	2570	/	/
S3	3 : 7	1000	2570	1110	56.8
S3	3 : 7	3000	2570	318	83.6

3. Results and Discussion

3.1. Performance Evaluation of Viscosity Reducer

3.1.1. Oil-Water Interfacial Tension Property. Viscosity reducer can play a role in reducing interfacial tension between water and oil. Lower interfacial tension can effectively reduce the adhesion work and capillary force, which can reduce the crude oil flow resistance and improve the oil displacement efficiency. Therefore, it is very important to study the interfacial tension between viscosity reducer and heavy oil. Texas-500c interfacial tension meter was used to measure the oil-water interfacial tension between three different viscosity reducers and degassed heavy oil in chen25 block of Shengli Oilfield by spinning drop method. The concentration of S1, S2, and S3 is 3000 $mg \cdot L^{-1}$, respectively. The measurement results are shown in Figure 2. The equilibrium interfacial tension between viscosity reducer S1 and heavy oil is the largest, 0.432 $mN \cdot m^{-1}$; S2 is the second, 0.0112 $mN \cdot m^{-1}$; and S3 is the lowest, 0.0031 $mN \cdot m^{-1}$.

3.1.2. The Emulsification Stability Evaluation. The key to heavy oil recovery is to improve the water-oil mobility ratio and improve the flow capacity of heavy oil in porous media. Viscosity reducer can disperse heavy oil in formation water to form O/W emulsion and effectively reduce the viscosity of crude oil. The stability of formed O/W emulsion can influence the viscosity reducing effect. The emulsification stability of a viscosity reducer is determined by the water separating proportion. The water separating proportion versus time of different viscosity reducers is depicted in Figure 3.

For three viscosity reducers S1 (10^{-1} $mN \cdot m^{-1}$), S2 (10^{-2} $mN \cdot m^{-1}$), and S3 (10^{-3} $mN \cdot m^{-1}$) with different magnitudes of interfacial tension, the water separating proportion increases until it is stable with the increase of time. The higher the water separating proportion is, the worse the stability of the emulsion is. For viscosity reducer S3, the water separating proportion exceeded 90% within 5 minutes, indicating that the stability of the emulsion is very poor, while the water separating proportion of S1 and S2 is significantly lower than that of S3, which has good stability. Moreover, the emulsifying stability of S1 is better than that of S2. The lower the interfacial tension is, the worse the emulsification stability is.

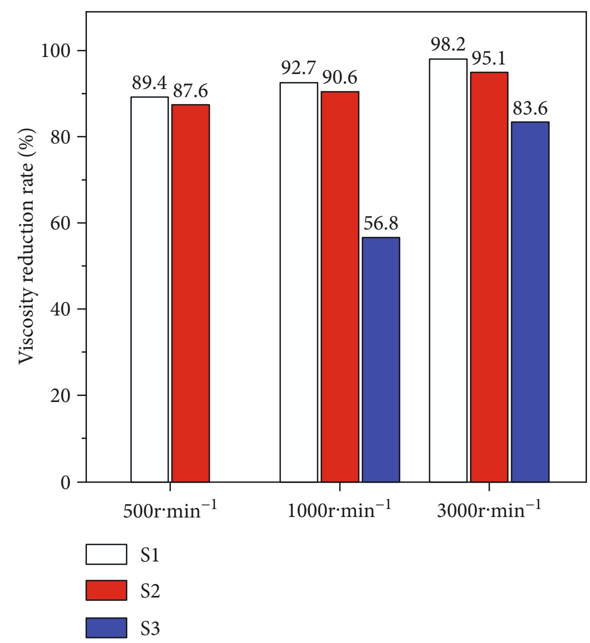

Figure 4: Viscosity reduction rate of three viscosity reducers at different shear rates at 70°C.

3.1.3. The Viscosity Reducing Ability Evaluation. Heavy oil is a typical non-Newtonian fluid; its viscosity is greatly affected by shear rate. Therefore, the viscosity reduction performance of the three viscosity reducers at different stirring speeds (500 $r \cdot min^{-1}$, 1000 $r \cdot min^{-1}$, and 3000 $r \cdot min^{-1}$) was evaluated. Table 3 and Figure 4 describe the viscosity reduction rates of the three viscosity reducers S1, S2, and S3 at different stirring speeds. The concentration of S1, S2, and S3 is 3000 $mg \cdot L^{-1}$, respectively.

When the stirring speed is 500 $r \cdot min^{-1}$, the emulsification stability of S3 emulsion is poor, and its viscosity reduction rate cannot be measured. When the viscosity reducer is constant, the viscosity reduction rate increases with the increase of stirring speed. When the stirring speed is constant, the viscosity reduction rates of S1 and S2 are significantly higher than that of S3. In general, the viscosity reduction rates of S1 and S2 at different stirring speeds are greater than 80%, while the viscosity reduction rate of S3 is more affected by the stirring speed.

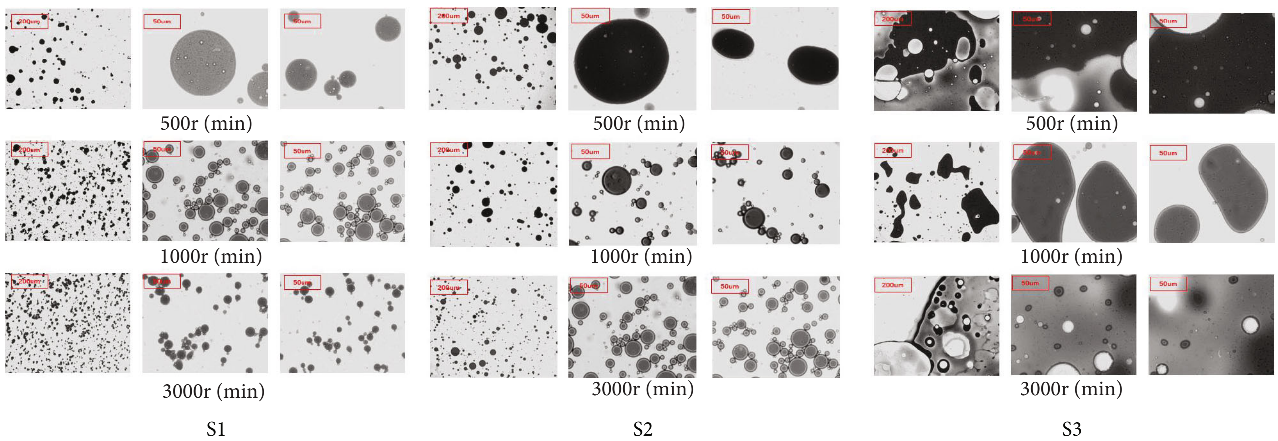

Figure 5: Microscopic images of heavy oil after emulsification by S1, S2, and S3.

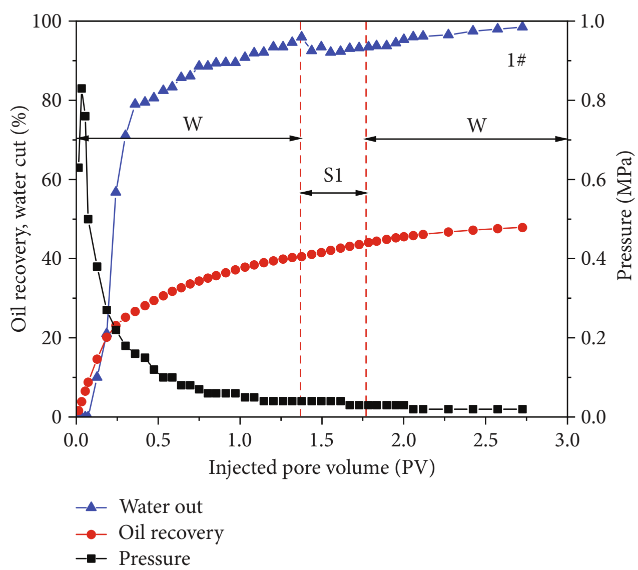

(a)

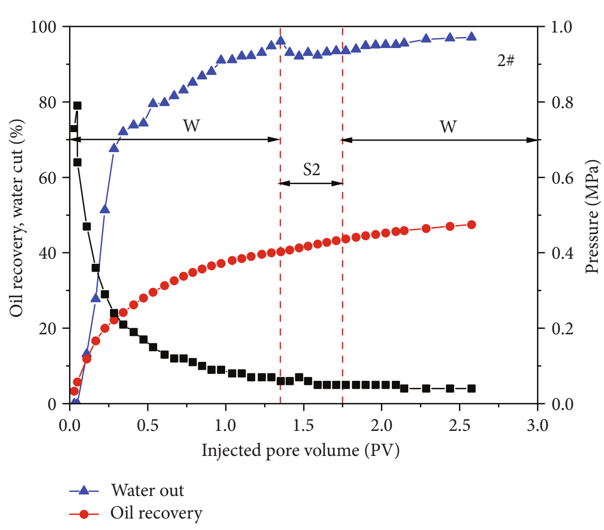

(b)

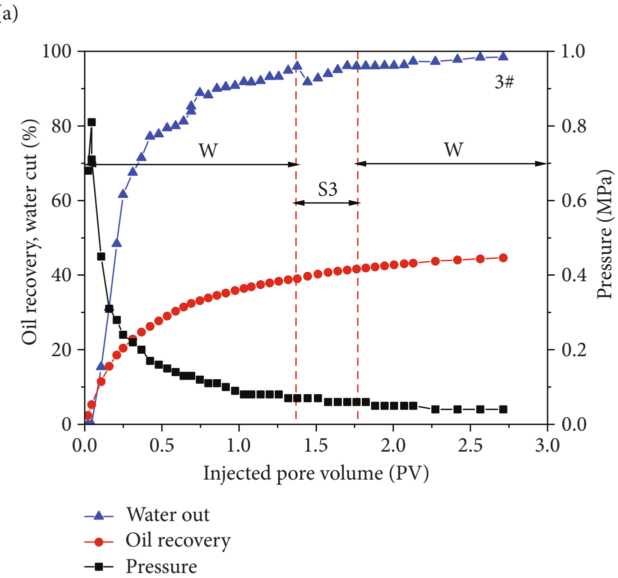

(c)

Figure 6: The oil recovery, water cut, and injection pressure versus pore volume: (a) S1 flooding; (b) S2 flooding; (c) S3 flooding.

Table 4: The incremental oil recovery results of viscosity reducer flooding at different flooding stages.

No.	Chemical slug	Water flooding recovery (%)	Chemical flooding recovery (%)	Incremental oil recovery (%)
1#	S1	40.6	47.9	7.3
2#	S2	40.3	47.8	7.5
3#	S3	39.1	44.7	5.6

3.1.4. The Morphology of Formed Emulsion Observation. The morphology of formed emulsion at different rotating speeds was studied by optical microscope. The microscopic images of emulsions formed by three viscosity reducers with different interfacial tensions are shown in Figure 5.

When the oil-water ratio is 3 : 7, 3000 mg·L^{-1} viscosity reducer S1 or S2 and heavy oil can form stable O/W emulsion under the conditions of 500 r·min^{-1}, 1000 r·min^{-1}, and 3000 r·min^{-1}, and the oil droplet size in the emulsion decreases with the increase of shear rate. Under the same shear rate, the oil droplet size in S1 emulsion is larger than that in S2. It shows that the emulsification and viscosity reduction performance of viscosity reducer S1 is better than S2, which is also consistent with the measurement results of the viscosity reduction rate in Section 3.1.2.

However, after fully mixing S3 and heavy oil at low shear rate, the morphology still showed oil block, oil mass, and oil-water separation. Until the shear rate reached 3000 r·min^{-1}, oil droplets can be observed in S3 emulsion, but the surface is still wrapped by an oil film, indicating that S3 has poor emulsifying ability and cannot make heavy oil reach a better emulsifying state.

Overall, the size of emulsion droplets varies significantly with the increase of stirring speed, and the size decreases with the increase of stirring speed. From the observation results, except S3, both S1 and S2 can form stable O/W emulsion, and the size of S2 is larger than S1, indicating that the emulsifying performance of S1 is better than S2 and S3, which is consistent with the evaluation results in Section 3.1.2. With the increase of stirring speed, the size decreases significantly and the number of small droplets increases, so that the dispersed phase is more evenly dispersed in the continuous phase. Therefore, compared with the viscosity of crude oil, the apparent viscosity of emulsion decreases sharply. The droplet size and dispersion effect of S1 and S2 emulsion are obviously better than that of S3, and the viscosity reduction effect of S3 is also the worst, which is consistent with the evaluation results of viscosity reduction rate in Section 3.1.3.

3.2. Enhanced Oil Recovery Ability

3.2.1. Analysis of Experimental Results of Viscosity Reducer Flooding. In order to study the ability of viscosity reducers with different interfacial tensions to improve the recovery of common heavy oil, a series of sand pack flooding experiments was carried out. The flooding curves of S1, S2, and S3 viscosity reducers are shown in Figure 6. The changes of injection pressure, water cut, and recovery with injection pore volume during viscosity reducer flooding with different interfacial tensions were analyzed.

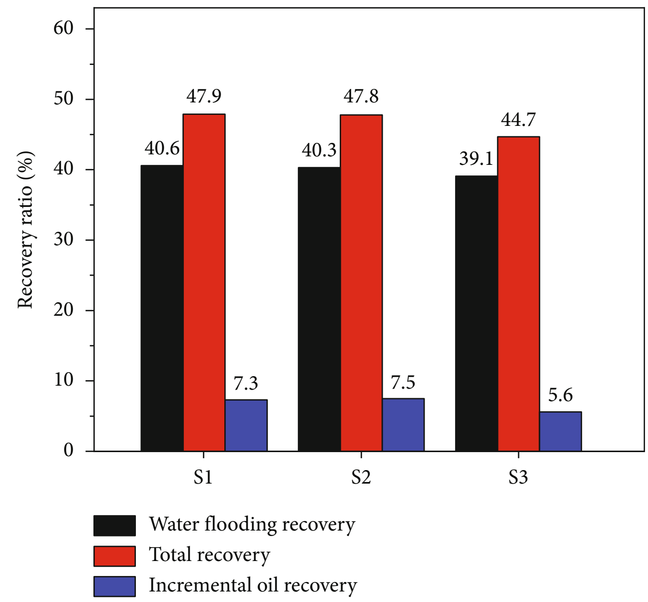

Figure 7: The incremental oil recovery results of viscosity reducer flooding at different flooding stages.

The flooding process is mainly divided into three stages: early water flooding stage, different chemical agent flooding stage, and subsequent water flooding stage. As shown in Figure 6, during the water flooding development stage, with the increase of injection pore volume, the injection pressure increases firstly and then decreases rapidly until it is stable after reaching the breakthrough pressure. The maximum pressure is in the range of 0.79 and 0.83 MPa, and the stable pressure of water flooding is in the range of 0.04~0.07 MPa. Moreover, with the increase of injected pore volume, the growth rate of water cut is fast in the early stage and slow in the later stage. When the injected pore volume is about 1.35 PV, the water cut reached 95%. The water flooding recovery is about 40%.

At the chemical flooding and subsequent water flooding stages, during the injection of three viscosity reducers with different interfacial tensions and subsequent water flooding, the injection pressure does not rise and decrease slowly until stable, and there is no decline funnel in the water cut curve. The final pressures of viscosity reducer flooding with different interfacial tensions of S1, S2, and S3 are 0.02 MPa, 0.03 MPa, and 0.04 MPa, respectively. In the process of viscosity reducer flooding, the pressure of S3 is slightly higher than that of S2 and S1, because S3 has the worst viscosity reduction performance and emulsification stability and the weakest ability to improve water-oil mobility ratio, so the flow resistance is also the largest in the flow process.

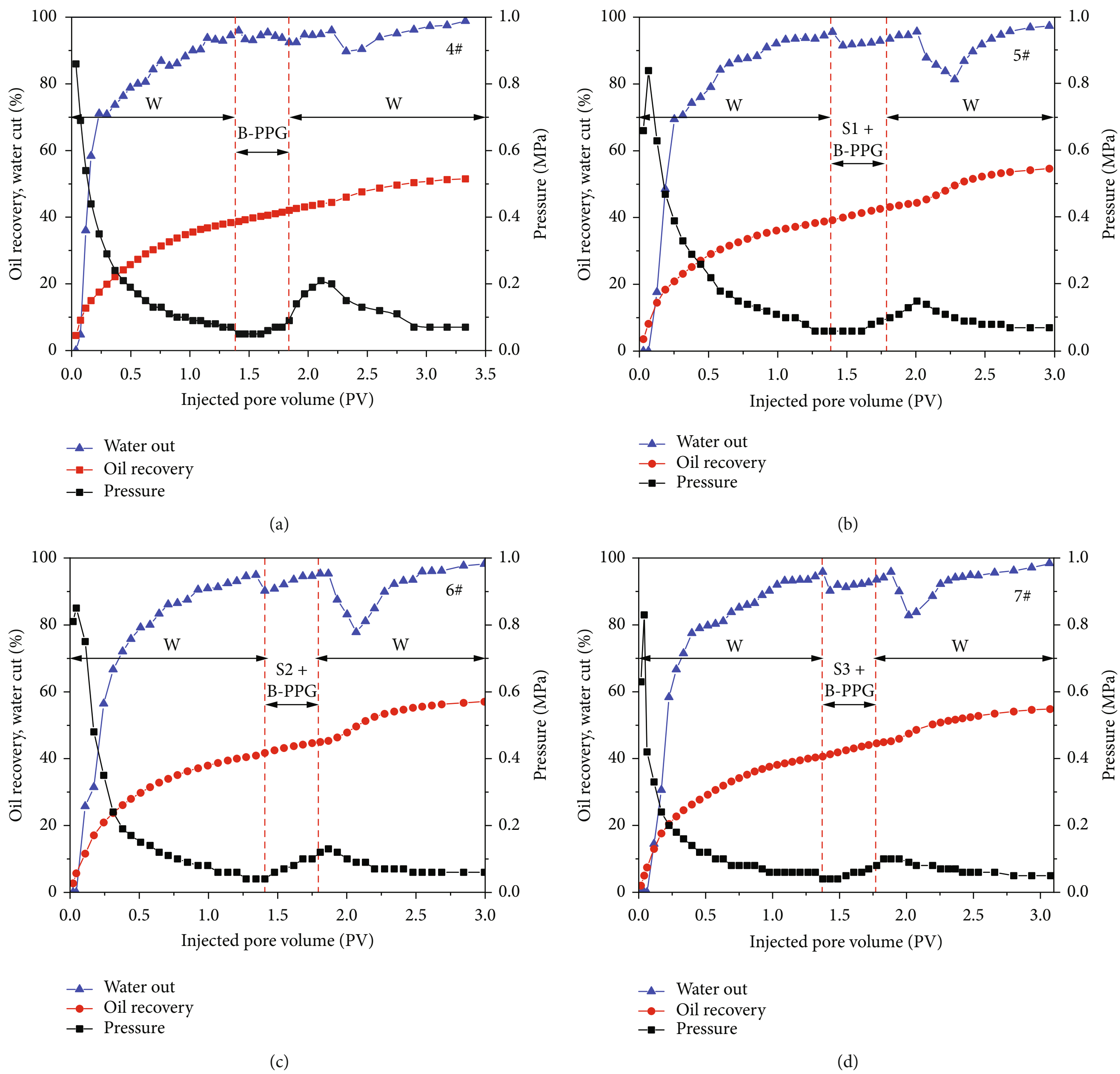

Figure 8: The oil recovery, water cut, and injection pressure versus pore volume: (a) B-PPG flooding; (b) S1/B-PPG flooding; (c) S2/B-PPG flooding; (d) S3/B-PPG flooding.

In order to further compare the EOR efficiency of three viscosity reducers with different interfacial tension, the incremental oil recovery of viscosity reducer flooding is analyzed, as shown in Table 4. The histogram of incremental oil recovery is drawn as shown in Figure 7. The incremental oil recovery of viscosity reducer S2 flooding is the largest, 7.5%, followed by S1, 7.3%, and S3, 5.6%. The results show that viscosity reducer S2 has the best ability to improve the recovery of common heavy oil. Viscosity reducer S2 not only has low interfacial tension and can effectively reduce adhesion work and improve oil displacement efficiency but also has good emulsification and viscosity reduction ability, can improve oil-water flow rate, and can enhance oil recovery.

3.2.2. Analysis of Experimental Results of B-PPG Flooding and Viscosity Reducer/B-PPG Composite Flooding. In the process of viscosity reducer flooding, water channeling is easy to occur, and most of the injected fluid flows out along the dominant channel, so the ability to improve the water-oil mobility ratio is limited. Therefore, the ability to improve the recovery of ordinary heavy oil for viscosity reducer flooding with different interfacial tensions is limited. In order to further compare the ability of three different interfacial tension viscosity reducers to enhance the recovery of ordinary heavy oil, a series of B-PPG flooding and viscosity reducer/B-PPG composite flooding experiments was carried out.

Table 5: The incremental oil recovery results of flooding at different flooding stages.

No.	Chemical slug	Water flooding recovery (%)	Chemical flooding recovery (%)	Incremental oil recovery (%)
4#	B-PPG	38.8	51.5	12.7
5#	S1+B-PPG	39.2	54.9	15.7
6#	S2+B-PPG	40.9	57.1	16.2
7#	S3+B-PPG	40.7	54.8	14.1

Figure 8(a) is the B-PPG flooding curve. Figures 8(b)–8(d) are the flooding curves of viscosity reducer with different interfacial tensions and B-PPG composite system. The flooding process is also divided into three parts. In the early stage of water injection development, the flooding curves are not significantly different. However, in the chemical flooding and subsequent water flooding stages, after injecting B-PPG or composite system, the injection pressure firstly increases and then decreases and finally tends to be stable. The water cut curve shows a downward funnel phenomenon, and the decline range of water cut curve of viscosity reducer/B-PPG composite flooding is more obvious. The reasons for this difference are as follows: In the process of viscosity reducer flooding, the viscosity reducer can enter along the dominant seepage channel formed by water flooding, and the injection pressure does not rise. Moreover, the viscosity reducer can peel off the remaining oil contacted after water flooding and reduce the seepage resistance, resulting in the slow reduction to stability of the injection pressure. In the process of B-PPG flooding or composite flooding, B-PPG will block the dominant seepage channel formed by water flooding. With the continuous injection of B-PPG and composite system, the injection pressure increases slowly. When the pressure rises to a certain extent, B-PPG will break or deform, and the subsequent pressure will decrease.

Moreover, during the subsequent water flooding stage, the peak pressure of the composite system is between 0.10 and 0.15 MPa, which is less than 0.21 MPa of the B-PPG flooding system. The reasons for this difference are that the emulsification and viscosity reduction performance of the viscosity reducer can reduce the flow resistance of heavy oil and reduce the pressure.

Table 5 and Figure 9 depict the incremental oil recovery of B-PPG flooding or viscosity reducer/B-PPG composite flooding at different stages. As shown in the figure, during the chemical flooding stage, the incremental oil recovery of B-PPG is 12.7%, while that of composite flooding is between 14.1 and 16.2%.

Compared with viscosity reducer flooding, B-PPG flooding has better EOR efficiency. In the process of viscosity reducer flooding, water channeling is easy to occur, most of the injected fluid flows out along the dominant channel, and the ability to improve the water-oil mobility ratio is limited. B-PPG can increase the viscosity of injection fluid and improve the water-oil mobility ratio. It can block the dominant seepage channel generated in the process of water flooding and expand the swept volume. The results show that the effect of improving water-oil mobility ratio and increasing sweep volume is greater than that of emulsification, viscosity reduction, and oil displacement efficiency.

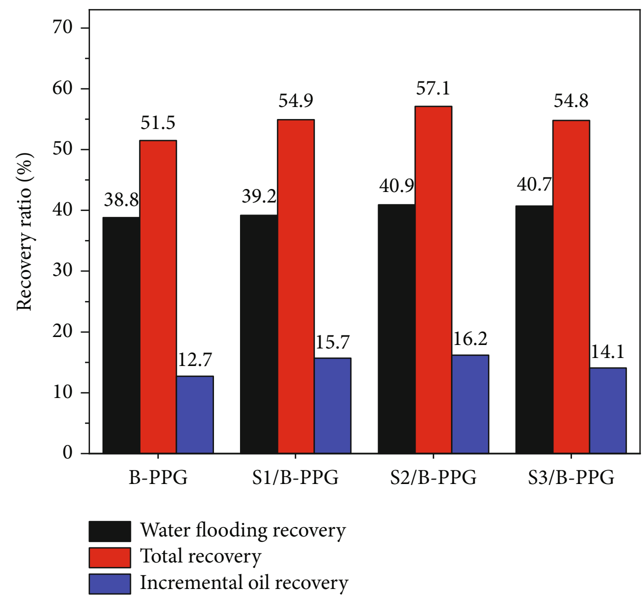

Figure 9: The incremental oil recovery results of flooding at different flooding stages.

Whether it is viscosity reducer flooding or viscosity reducer/B-PPG composite flooding, the ability of emulsion oriented S1 to improve the recovery of ordinary heavy oil is significantly better than that of low interfacial tension viscosity reducer S3, indicating that the mechanism of emulsion viscosity reduction and displacement is more critical than low interfacial tension for recovering ordinary heavy oil reservoir. The incremental oil recovery of S2 is higher than that of emulsified viscosity reducer S1, which shows that the viscosity reducer with low interfacial tension has better EOR effect when the emulsifying capacity and viscosity reducing performance are similar.

4. Conclusions

In this study, a series of experiments including physicochemical property evaluation of viscosity reducer and B-PPG and sand pack flooding experiments was systematically conducted to investigate the EOR ability of three different viscosity reducers, B-PPG, and viscosity reducer/B-PPG composite systems. Some main conclusions can be drawn as follows:

(1) The oil-water interfacial tensions of the three viscosity reducers S1, S2, and S3 are 0.432 $mN \cdot m^{-1}$, 0.0112 $mN \cdot m^{-1}$, and 0.0031 $mN \cdot m^{-1}$, respectively. S1 with the highest interfacial tension has the best

emulsification and viscosity reduction performance, S2 is the second, and S3 is the worst. The lower the interfacial tension, the worse the emulsification stability and the worse the viscosity reduction performance

(2) S2 with moderate interfacial tension and emulsifying capacity has the best EOR efficiency, followed by S1 with the highest interfacial tension and the best emulsifying performance and the recovery increment of S3 with the lowest interfacial tension, and the worst emulsification performance is the smallest. The emulsion viscosity reduction is more important than lowering interfacial tension for viscosity reducer to improve oil recovery of ordinary heavy oil

(3) The incremental oil recovery of B-PPG is 12.7%, which is significantly higher than that of viscosity reducer flooding. Compared with viscosity reducer flooding, the viscosity reducer/B-PPG composite systems have better EOR capacity. For enhancing oil recovery of ordinary heavy oil reservoir, the effect of improving water-oil mobility ratio and increasing sweep volume is greater than that of emulsification, viscosity reduction, and oil displacement efficiency

Data Availability

All data used to support the findings of this study are available from the corresponding author on request.

Conflicts of Interest

The author declares that there are no conflicts of interest.

Acknowledgments

The research was financially supported by the Research Institute of Exploration and Development of Shengli Oilfield, SINOPEC.

References

[1] A. Mai, J. Bryan, N. Goodarzi, and A. Kantzas, "Insights into non-thermal recovery of heavy oil," *Journal of Canadian Petroleum Technology*, vol. 48, no. 3, pp. 27–35, 2009.

[2] V. Alvarado and E. Manrique, "Enhanced oil recovery: an update review," *Energies*, vol. 3, no. 9, pp. 1529–1575, 2010.

[3] B. Su and Y. Fujimitsu, "Research on heavy oil thermal recovery by CO_2 steam flooding with help of combination of borehole-surface electric potential and cross-borehole electric potential," *Energy Exploration and Exploitation*, vol. 29, no. 6, pp. 797–815, 2011.

[4] T. Babadagli and B. Ozum, "BioDiesel as additive in high pressure and temperature steam recovery of heavy oil and bitumen," *Oil & Gas Science and Technology – Revue d'IFP Energies nouvelles*, vol. 67, no. 3, pp. 413–421, 2012.

[5] S. Huang, M. Cao, and L. Cheng, "Experimental study on the mechanism of enhanced oil recovery by multi-thermal fluid in offshore heavy oil," *International Journal of Heat and Mass Transfer*, vol. 122, pp. 1074–1084, 2018.

[6] O. A. Alomair and A. F. Alajmi, "A novel experimental nanofluid-assisted steam flooding (NASF) approach for enhanced heavy oil recovery," *Fuel*, vol. 313, article 122691, 2022.

[7] S. Li, Z. Li, and X. Sun, "Effect of flue gas and n-hexane on heavy oil properties in steam flooding process," *Fuel*, vol. 187, pp. 84–93, 2017.

[8] G. Z. Liao, H. Z. Wang, Z. M. Wang et al., "Oil oxidation in the whole temperature regions during oil reservoir air injection and development methods," *Petroleum Exploration and Development*, vol. 47, no. 2, pp. 357–364, 2020.

[9] W. F. Pu, H. Gao, Y. B. Li, and Q. Luo, "Performance and mechanisms of enhanced oil recovery via CO_2 assisted steam flooding technique in high heterogeneity heavy oil reservoir: PVT and 3D experimental studies," *Petroleum Science and Technology*, vol. 38, no. 15, pp. 823–835, 2020.

[10] G. Feng, Y. Li, and Z. Yang, "Performance evaluation of nitrogen-assisted steam flooding process in heavy oil reservoir via numerical simulation," *Journal of Petroleum Science and Engineering*, vol. 189, article 106954, 2020.

[11] Z. Pang, Y. Jiang, B. Wang, G. Cheng, and X. Yu, "Experiments and analysis on development methods for horizontal well cyclic steam stimulation in heavy oil reservoir with edge water," *Journal of Petroleum Science and Engineering*, vol. 188, article 106948, 2020.

[12] E. Luo, Z. Fan, Y. Hu et al., "An efficient optimization framework of cyclic steam stimulation with experimental design in extra heavy oil reservoirs," *Energy*, vol. 192, article 116601, 2020.

[13] L. Shi, X. Li, C. Xi, Z. Qi, and P. Liu, "Analytical modeling of the oil steam ratio during the lifetime steam-assisted gravity drainage process in extra-heavy oil reservoirs," *Journal of Petroleum Science and Engineering*, vol. 203, article 108616, 2021.

[14] D. W. Zhao, J. Wang, and I. D. Gates, "Optimized solvent-aided steam-flooding strategy for recovery of thin heavy oil reservoirs," *Fuel*, vol. 112, pp. 50–59, 2013.

[15] Y. Zhao, "Laboratory experiment and field application of high pressure and high quality steam flooding," *Journal of Petroleum Science and Engineering*, vol. 189, article 107016, 2020.

[16] P. Li, F. Zhang, T. Zhu, C. Zhang, G. Liu, and X. Li, "Synthesis and properties of the active polymer for enhanced heavy oil recovery," *Colloids and Surfaces A: Physicochemical and Engineering Aspects*, vol. 626, article 127036, 2021.

[17] A. O. Ezzat, A. M. Atta, H. A. al-Lohedan, and A. I. Hashem, "Synthesis and application of new surface active poly (ionic liquids) based on 1,3-dialkylimidazolium as demulsifiers for heavy petroleum crude oil emulsions," *Journal of Molecular Liquids*, vol. 251, pp. 201–211, 2018.

[18] A. M. Hassan, M. Ayoub, M. Eissa, H. Bruining, and P. Zitha, "Study of surface complexation modeling on a novel hybrid enhanced oil recovery (EOR) method; smart-water assisted foam-flooding," *Journal of Petroleum Science and Engineering*, vol. 195, article 107563, 2020.

[19] L. Shi, C. Liu, M. Chen, Z. Hua, and J. Zhang, "Synthesis and evaluation of a hyperbranched copolymer as viscosity reducer for offshore heavy oil," *Journal of Petroleum Science and Engineering*, vol. 196, article 108011, 2021.

[20] Y. Gong and Y. Gu, "Miscible CO_2 simultaneous water-and-gas (CO_2-SWAG) injection in the Bakken formation," in *SPE*

CSUR Unconventional Resources Conference, Calgary, Alberta, Canada, 2015.

[21] Y. Gong and Y. Gu, "Experimental study of water and CO_2 flooding in the tight main pay zone and vuggy residual oil zone of a carbonate reservoir," *Energy & Fuels*, vol. 29, no. 10, pp. 6213–6223, 2015.

[22] L. Xue, P. Liu, and Y. Zhang, "Development and Research Status of Heavy Oil Enhanced Oil Recovery," *Geofluids*, vol. 2022, Article ID 5015045, 13 pages, 2022.

[23] X. Wang, W. Liu, L. Shi et al., "Application of a novel amphiphilic polymer for enhanced offshore heavy oil recovery: mechanistic study and core displacement test," *Journal of Petroleum Science and Engineering*, vol. 215, article 110626, 2022.

[24] X. Gu, Y. Li, J. Yan, J. Zhang, and G. Chen, "Synthesis and investigation of a spiro diborate as a clean viscosity-reducer and pour point depressor for crude oil," *Petroleum Chemistry*, vol. 59, no. 6, pp. 570–574, 2019.

[25] F. Zhang, Y. Liu, Q. Wang, Y. Han, and Y. Tan, "Fabricating a heavy oil viscosity reducer with weak interaction effect: synthesis and viscosity reduction mechanism," *Colloids and Interface Science Communications*, vol. 42, article 100426, 2021.

[26] H. Sun, Z. Wang, Y. Sun, G. Wu, B. Sun, and Y. Sha, "Laboratory evaluation of an efficient low interfacial tension foaming agent for enhanced oil recovery in high temperature flue-gas foam flooding," *Journal of Petroleum Science and Engineering*, vol. 195, article 107580, 2020.

[27] X. Jiang, M. Liu, X. Li, L. Wang, S. Liang, and X. Guo, "Effects of surfactant and hydrophobic nanoparticles on the crude oil-water interfacial tension," *Energies*, vol. 14, no. 19, p. 6234, 2021.

[28] A. K. Manshad, M. Rezaei, S. Moradi, I. Nowrouzi, and A. H. Mohammadi, "Wettability alteration and interfacial tension (IFT) reduction in enhanced oil recovery (EOR) process by ionic liquid flooding," *Journal of Molecular Liquids*, vol. 248, pp. 153–162, 2017.

[29] X. Wang, H. Zhang, X. Liang, L. Shi, and Z. Ye, "New amphiphilic macromolecule as viscosity reducer with both asphaltene dispersion and emulsifying capacity for offshore heavy oil," *Energy & Fuels*, vol. 35, no. 2, pp. 1143–1151, 2021.

[30] S. J. D. Sofla, M. Sharifi, and A. H. Sarapardeh, "Toward mechanistic understanding of natural surfactant flooding in enhanced oil recovery processes: the role of salinity, surfactant concentration and rock type," *Journal of Molecular Liquids*, vol. 222, pp. 632–639, 2016.

[31] O. S. Alade, D. Al Shehri, M. Mahmoud et al., "A novel technique for heavy oil recovery using poly vinyl alcohol (PVA) and PVA-NaOH with ethanol additive," *Fuel*, vol. 285, article 119128, 2021.

[32] H. Azarhava, A. Jafari, F. Vakilchap, and S. M. Mousavi, "Stability and performance of poly γ-(glutamic acid) in the presence of sulfate ion for enhanced heavy oil recovery," *Journal of Petroleum Science and Engineering*, vol. 196, article 107688, 2021.

[33] Y. Chen, H. He, Q. Yu, H. Liu, and W. Liu, "Insights into enhanced oil recovery by polymer-viscosity reducing surfactant combination flooding in conventional heavy oil reservoir," *Geofluids*, vol. 2021, Article ID 7110414, 12 pages, 2021.

[34] L. F. Lamas, V. E. Botechia, D. J. Schiozer, M. L. Rocha, and M. Delshad, "Application of polymer flooding in the revitalization of a mature heavy oil field," *Journal of Petroleum Science and Engineering*, vol. 204, article 108695, 2021.

[35] W. Song and D. G. Hatzignatiou, "On the reduction of the residual oil saturation through the injection of polymer and nanoparticle solutions," *Journal of Petroleum Science and Engineering*, vol. 208, article 109430, 2021.

[36] K. Medica, R. Maharaj, D. Alexander, and M. Soroush, "Evaluation of an alkali-polymer flooding technique for enhanced oil recovery in Trinidad and Tobago," *Journal of Petroleum Exploration and Production Technology*, vol. 10, no. 8, pp. 3947–3959, 2020.

[37] P. Ghosh and K. K. Mohanty, "Study of surfactant-polymer flooding in high-temperature and high-salinity carbonate rocks," *Energy & Fuels*, vol. 33, no. 5, pp. 4130–4145, 2019.

[38] F. Rezaeiakmal and R. Parsaei, "Visualization study of polymer enhanced foam (PEF) flooding for recovery of waterflood residual oil: effect of cross flow," *Journal of Petroleum Science and Engineering*, vol. 203, article 108583, 2021.

[39] M. Kokubun, F. A. Radu, E. Keilegavlen, K. Kumar, and K. Spildo, "Transport of polymer particles in oil-water flow in porous media: enhancing oil recovery," *Transport in Porous Media*, vol. 126, no. 2, pp. 501–519, 2019.

[40] R. Farajzadeh, A. Ameri, M. J. Faber, D. W. van Batenburg, D. M. Boersma, and J. Bruining, "Effect of continuous, trapped, and flowing gas on performance of alkaline surfactant polymer (ASP) flooding," *Industrial & Engineering Chemistry Research*, vol. 52, no. 38, pp. 13839–13848, 2013.

[41] M. A. Kalbani, M. Jordan, E. Mackay, K. Sorbie, and N. Long, "Modelling the impact of alkaline-surfactant and alkaline-surfactant-polymer flooding processes on scale precipitation and management," *Journal of Petroleum Science and Engineering*, vol. 205, article 108777, 2021.

[42] A. Davarpanah and B. Mirshekari, "Numerical simulation and laboratory evaluation of alkali–surfactant–polymer and foam flooding," *International journal of Environmental Science and Technology*, vol. 17, no. 2, pp. 1123–1136, 2020.

[43] A. Aitkulov and K. K. Mohanty, "Investigation of alkaline-surfactant-polymer flooding in a quarter five-spot sandpack for viscous oil recovery," *Journal of Petroleum Science and Engineering*, vol. 175, pp. 706–718, 2019.

[44] Z. Li, Y. Wang, H. He, F. Yuan, and Y. Chen, "Insights into the effects of salinity on the transport behavior of polymer-enhanced branched-preformed particle gel suspension in porous media," *Energy & Fuels*, vol. 35, no. 2, pp. 1104–1112, 2021.

[45] H. He, W. Liu, Y. Chen, H. Liu, H. Liu, and G. Luo, "Synergistic mechanism of well pattern adjustment and heterogeneous phase combined flooding on enhancing oil recovery in mature fault-block reservoirs," *Journal of Petroleum Exploration and Production Technology*, vol. 12, no. 12, pp. 3387–3398, 2022.

[46] W. Liu, H. He, F. Yuan et al., "Influence of the injection scheme on the enhanced oil recovery ability of heterogeneous phase combination flooding in mature waterflooded reservoirs," *ACS Omega*, vol. 7, no. 27, pp. 23511–23520, 2022.

[47] W. Zhu, B. Li, Y. Liu, H. Song, M. Yue, and N. Wu, "A new calculating method for relative permeability of branched preformed particle gel flooding in multiphase composite system," *Special Topics & Reviews in Porous Media*, vol. 10, no. 1, pp. 89–98, 2019.

[48] Q. J. Du, G. M. Pan, J. Hou, L. L. Guo, R. R. Wang, and Z. Z. Xia, "Study of the mechanisms of streamline-adjustment-

assisted heterogeneous combination flooding for enhanced oil recovery for post-polymer-flooded reservoirs," *Petroleum Science*, vol. 16, no. 3, pp. 606–618, 2019.

[49] H. He, J. Fu, B. Hou et al., "Investigation of injection strategy of branched-preformed particle gel/polymer/surfactant for enhanced oil recovery after polymer flooding in heterogeneous reservoirs," *Energies*, vol. 11, no. 8, p. 1950, 2018.

[50] M. O. Elsharafi and B. Bai, "Effect of weak preformed particle gel on unswept oil zones/areas during conformance control treatments," *Industrial & Engineering Chemistry Research*, vol. 51, pp. 11547–11554, 2013.

[51] B. Bai, L. Li, Y. Liu, H. Liu, Z. Wang, and C. You, "Preformed particle gel for conformance control: factors affecting its properties and applications," *SPE Reservoir Evaluation & Engineering*, vol. 10, no. 4, pp. 415–422, 2007.

[52] L. Xu, Z. Qiu, H. Gong et al., "Synergy of microbial polysaccharides and branched-preformed particle gel on thickening and enhanced oil recovery," *Chemical Engineering Science*, vol. 208, article 115138, 2019.